DEUTSCHES ELEKTRONEN-SYNCHROTRON DESY

DESY 72/59
October 1972

Multi-Regge Exchange and Eikonalization

by

Jochen Bartels

II. Institut für Theoretische Physik der Universität Hamburg
and
Deutsches Elektronen-Synchrotron DESY, Hamburg

2 HAMBURG 52 · NOTKESTIEG 1

Multi-Regge-Exchange and Eikonalization

by

Jochen Bartels
II. Institut für Theoretische Physik der Universität Hamburg
and
Deutsches Elektronen-Synchrotron DESY, Hamburg

Abstract

The Regge-eikonal model in ϕ^3-theory is studied within the framework of the impact-picture of Cheng and Wu or, equivalently, the reggeon calculus of Gribov. The exchanged reggeons are Bethe-Salpeter amplitudes in the ladder approximation and thus contain all orders of the coupling constant in the vertex function and trajectory function. This gives a more detailed insight into eikonalization than earlier studies, where the exchanged ladders were taken only in the weak-coupling limit. We find - in contrast to earlier studies - that not all permutations of the reggeon legs to the external particles are equally important, but a certain subgroup of them dominates. Furthermore, we see that the situation of eikonalization in the weak-coupling limit of the ladders is quite different from the more general case, where vertex- and trajectory-functions contain all orders of the coupling-constant.

I. Introduction

In recent years there have been several attempts to justify within simple field-theoretic models the eikonal form for the elastic scattering amplitude. For QED and ϕ^3 it is shown[1] that in the high-energy limit certain contributions of the generalized ladder diagrams give the eikonal form. In these contributions the large momenta pass the diagram through the straight lines of the ladder, and these paths are therefore called the eikonal paths. In QED these contributions are the dominant ones for large s, while in ϕ^3 they are not.

But since the eikonal scattering amplitude is often used as a model for Regge-cuts, phenomenologists are more interested in a study of Feynman diagrams, in which more complicated objects such as reggeons are exchanged, e.g. ladders in ϕ^3 and towers in QED. Usually one studies such Feynman diagrams in this way: for each power of the coupling constant one finds the coefficient of the highest power of $\ln s$ and then sums over all orders of the coupling constant. For QED such a study was made in [2] and [3]: the authors used infinite-momentum techniques, and they found that in fact for tower-exchange the eikonal form emerges for high energies. In ϕ^3 only the two-reggon exchange, namely the Mandelstam diagram has an eikonal high-energy limit, while for the exchange of more than two ladders this does not hold. Only when one confines oneself to the contributions of the eikonal paths in these diagrams, one gets the eikonal form as well, similarly to the situation with generalized ladders described above. But in ϕ^3 this is not the true high-energy limit. These results on ϕ^3 stem from[4)-8)], but there are different statements on the question which structures of reggeon coupling to the external particle actually contribute (cf. Ref.4) and 6)).

But there is no reason to assume that the sum of the coefficients of only the leading powers of $\ln s$ gives the true high-energy limit of the whole sum. What one actually finds in this way is the high-energy form of the sum in the limit of a very small coupling constant. Thus the results on eikonalization proved with methods as those described above, are valid only for reggeons which are taken in the weak coupling limit but not for physical reggeons. Nevertheless, the weak coupling limit for the reggeon amplitude can be rather different from the full amplitude: for instance, in the case of ϕ^3-ladders, the reggeon-vertex functions are simply constants[9] in the weak coupling limit, while the full functions

are assumed to have cuts in the momentum-transfer and in the external masses. So one might expect that the situation of eikonalization changes if one goes beyond the weak coupling limit.

A possibility to overcome the limitation of the weak coupling limit is to take for the exchanged reggeons a closed representation, which contains all orders of the coupling constant and whose analytic properties in momentum transfer and masses are known. This was done for ϕ^3 by Cheng and Wu[10]. They took the full Bethe-Salpeter amplitude for the exchanged reggeons and found that in fact the eikonal high-energy limit of the Mandelstam diagram holds only in the weak coupling limit, but breaks down if one goes beyond the weak coupling limit.

The aim of our paper is to study the exchange of an arbitrary number of ladders in ϕ^3, for which we take Bethe-Salpeter amplitudes, similarly to Ref.10, where only the Mandelstam diagram was considered in detail. We start with the impact picture of Cheng and Wu[10], as the general form for the multi-Regge exchange in the high energy limit. In our case this is completely equivalent to the reggeon calculus developed by Gribov[13]. For the single reggeon we make a spectral ansatz, which allows a detailed study of the impact factors or the Gribov-vertices. Since we know that eikonalization cannot be the high-energy form in ϕ^3, we concentrate on the question of the mechanism of eikonalization. Our neglect to ask for the exact high-energy behavior in perturbation theory may be justified by regarding the ϕ^3-model only as a very simple form of a field theory, which nevertheless shows already features of more realistic theories. So the study of ϕ^3 in our case will be a step towards a better understanding of the corresponding situation in QED.

Our results will be the following. Firstly, we shall show under what conditions eikonalization occurs, i.e. under what conditions the impact factors, which are in general multidimensional integrals over internal momenta, factorize into a simple product of reggeon-vertex functions. The essential step is the definition of the eikonal path through the vertices, and exactly in the weak-coupling limit of the exchanged ladders such a path is marked out. This is essentially a generalization of Ref.10 to an arbitrary number of reggeons, but we think that our spectral form is more suitable than the form used in [10]. The second result answers the question which structures in reggeon coupling to the external particles are necessary for eikonalization. This is still an

open question, because the statements in the literature disagree: in Ref.4 all permutations of the reggeon-legs to the external particles are taken into account, while in Ref.6 only a subgroup of permutations is used. We will find that the last result is valid only in the weak-coupling limit, while in the general case a larger subgroup of permutations, but not all permutations are used.

The plan of our paper is: at first we shall explain our framework of investigation, infinite-momentum techniques and the spectral ansatz for the reggeon. Then we look at two-reggeon exchange, in order to demonstrate the mechanism of eikonalization. The results for an arbitrary number of exchanged reggeons are given in Section III, details in Appendix A. In the fourth part we pass on to the weak coupling limit in order to get contact to the results of Ref.4-8 and see in which way the weak coupling limit changes the situation of eikonalization as compared to the general case. The last section is devoted to the question which structures of impact factors dominate for high energies. Summarizing remarks will conclude the paper.

II. Two-Reggeon-Exchange

As a starting point of our study of the high-energy behavior of diagrams with reggeon-exchange we use the results of Cheng und Wu[12], who found that in QED and ϕ^3 the high-energy behavior for the elastic scattering by exchange of n objects has the form (Fig.1):

$$T(s,t)\sim\int d^2q_1\ldots d^2q_n\,\delta^{(2)}(\Sigma q_{i_\perp}-(p_1-p_1)_\perp)\;I_1(q_{1_\perp},\ldots q_{n_\perp})\cdot I_2(q_{1_\perp},\ldots q_{n_\perp})\;P_1(q_{1_\perp})\ldots P_n(q_{n_\perp}) \tag{2.1}$$

where J_1 and J_2 are the impact factors of particles 1 and 2 and the P_i are the propagators of the exchanged objects, depending only on two-dimensional transverse momenta. In writing down the expressions for the impact factors which are determined by the structure of the upper and lower vertices, one takes the infinite-momentum variables $(p_o,\vec{p}) \to (p_+=p_o+p_3, p_-=p_o-p_3, \vec{p}_\perp)$. Thus one may neglect, within the upper vertex where the incoming particle has a large "+" component, all the "+" components of the exchanged particles momenta relative to the other "+" components occurring in the upper vertex. The same holds for the "-" components in the lower vertex. This results in a decoupling of the impact factors with respect to the "+" and "-" components of the q_i-momenta. Essentially the same was suggested by Gribov [13] and Winbow [14], although formulated in terms of Sudakov-variables. They justify this by means of damping properties of the amplitude of the exchanged objects for large values of the

momentum transfer and the external masses.

For the exchanged objects we take reggeon amplitudes, which could be simple ladders. But in order to be more general, we assume only factorization properties of the vertex function and make for each vertex part a spectral ansatz, which contains dependence on momentum transfer and external masses:

$$R(p_1^2,p_1'^2,p_2^2,p_2'^2;s,t) = b(p_1^2,p_1'^2;t)\ s^{\alpha(t)}\ \xi(t)\ b(p_2^2,p_2'^2;t) \qquad (2.2)$$
$$\xi(t)=1+e^{-i\pi\alpha(t)}$$

$$b(p_1^2,p_1'^2;t) = \int_{-1}^{+1} dz \int_{\gamma_0}^{\infty} d\gamma \frac{\bar{\varrho}(\gamma,z)}{\gamma-\frac{1+z}{2}p_1^2-\frac{1-z}{2}p_1'^2+\frac{1-z^2}{4}t-i\varepsilon} \qquad (2.3)$$

$$b(p_1^2,p_1'^2;t)\cdot(p_1^2-m_r^2)^{-1}\cdot(p_1'^2-m_r^2)^{-1}$$
$$= \int_{-1}^{+1} dz \int_{\gamma_0}^{\infty} d \frac{\varrho(\gamma,z)}{(\gamma-\frac{1+z}{2}p_1^2-\frac{1-z}{2}p_1'^2+\frac{1-z^2}{4}t-i\varepsilon)^3} \qquad (2.4)$$
$$= \int dZ \frac{\varrho(\gamma,z)}{(\gamma-\frac{1+z}{2}p_1^2-\frac{1-z}{2}p_1'^2+\frac{1-z^2}{4}t-i\varepsilon)^3}$$

We found this form more convenient than that of Ref.10). This spectral ansatz is justified at least for the ladder case [15)16)], and we assume it to be a more general one.

First we take the amplitude for the exchange of two reggeons (Fig.2a), which for ladder exchange would be the Mandelstam diagram:

$$T(s,t) = 2is(2\pi)^2\left(\frac{-i}{8\pi^2 s}\right)^2 \int d^2q\ (I_{2a}(r_{1\perp},q_\perp))^2\ s^{\alpha(-(r_1+q)_\perp^2)} \qquad (2.5)$$
$$\cdot\xi(-(r_1+q)_\perp^2)\cdot s^{\alpha(-(r_1-q)_\perp^2)}\cdot\xi(-(r_1-q)_\perp^2)$$

Evaluating the impact factors we start with the upper vertex, introducing the infinite-momentum variables for the q-momentum and approximating the reggeon-energies:

$$I_{2a}(r_{1\perp},q_\perp) = \left(\frac{ig^2}{(2\pi)^4}\right)^2 \int \frac{dq_-}{-2\pi i} \int d^4p_1 d^4p_2 \left(\frac{p_{1+}}{2\omega}\right)^{\alpha(-(r_1+q)_\perp^2)} \left(\frac{p_{2+}}{2\omega}\right)^{\alpha(-(r_1-q)}$$

$$\cdot \frac{1}{(r_1-p_1)^2-m^2} \frac{1}{(r_2-p_1-p_2-q)^2-m^2} \frac{1}{(r_2+r_1-p_1-q)^2-m^2}$$

$$\cdot \int dz_1 \frac{\varphi(\gamma_1,z_1)}{\left(\gamma_1-\frac{1+z_1}{2}(p_1-r_1)^2-\frac{1-z_1}{2}(p_1+q)^2+\frac{1-z_1^2}{4}(r_1+q)^2\right)^3} \qquad (2.6)$$

$$\cdot \int dz_2 \frac{\varphi(\gamma_2,z_2)}{\left(\gamma_2-\frac{1+z_2}{2}(p_2+q)^2-\frac{1-z_2}{2}(p_2+r_1)^2+\frac{1-z_2^2}{4}(r_1-q)^2\right)^3}$$

Now we introduce the notations:

$$(r_2)_z=-(r_3)_z\sim\omega+\frac{1}{2\omega}(r_1^2+m^2)=\omega+\frac{M^2}{2\omega}$$

$$(r_2)_+=(r_3)_-=2\omega$$

$$(r_2)_-=(r_3)_+=\frac{M^2}{2\omega}$$

$$(r_1)_o=(r_1)_z=0$$

$$(p_i)_+=2\omega x_i, \quad 2\omega(p_i)_-=y_i$$

$$2\omega(q)_-=y$$

From the y-integration one has the condition that there must always be singularities in both the upper and the lower half planes. This limits the x_i-integration to the intervals $0<x_i<1$, $i = 1,2$, $0<x_1+x_2<1$. Now we neglect everywhere q_+ and use for the reggeon-denominators the representation:

$$\frac{1}{(D-i\varepsilon)^3} = -\frac{i}{2}\int_0^\infty d\omega\,\omega^2\, e^{-i\omega D} \qquad (2.7)$$

Performing the y-integration gives:

$$I_{2a}=$$

$$\left(\frac{g^2}{2(2\pi)^3}\right)^2 \int d^2p_{1\perp} d^2p_{2\perp} \int_0^1 dx_1 \int_0^{1-x_1} dx_2 \frac{x_1^{\alpha(-(r_1+q)_\perp^2)}\; x_2^{\alpha(-(r_1-q)_\perp^2)}}{(1-x_1)^2(1-x_1-x_2)}$$

$$\cdot \int dz_1 dz_2 \varrho(\gamma_1, z_1)\cdot\varrho(\gamma_2, z_2)\cdot\left(-\frac{i}{2}\right)^2 \int_0^\infty d\omega_1\omega_1^2 d\omega_2\omega_2^2 e^{-i\omega_1 D_{1e}^a - i\omega_2 D_2^a} \qquad (2.8)$$

$$\cdot \theta\left(\omega_1 x_1 \frac{1+z_1}{2} - \omega_2 x_2 \frac{1+z_2}{2}\right)\cdot\theta\left(\omega_1 x_1 \frac{1-z_1}{2} - \omega_2 x_2 \frac{1-z_2}{2}\right)$$

with the notations

$$D_1^a = D_1 - x_1\frac{1+z_1}{2}\left(M^2 - \frac{(r_2-p_1)_\perp^2+m^2}{1-x_1}\right) - x_1\frac{1-z_1}{2}\left(M^2 - \frac{(r_1-p_1-q)_\perp^2+m^2}{1-x_1}\right)$$

$$D_2^a = D_2 - x_2\frac{1+z_2}{2}\left(\frac{(r_2-p_1)_\perp^2+m^2}{1-x_1} - \frac{(p_1+p_2+q)_\perp^2+m^2}{1-x_1-x_2}\right)$$

$$- x_2\frac{1-z_2}{2}\left(\frac{(r_1-p_1-q)_\perp^2+m^2}{1-x_1} - \frac{(p_1+p_2+q)_\perp^2+m^2}{1-x_1-x_2}\right)$$

$$D_1 = \gamma_1 + \frac{1+z_1}{2}(p_1-r_1)_\perp^2 + \frac{1-z_1}{2}(p_1+q)_\perp^2 - \frac{1-z_1^2}{4}(r_1+q)_\perp^2$$

$$D_2 = \gamma_2 + \frac{1+z_2}{2}(p_2+q)_\perp^2 + \frac{1-z_2}{2}(p_1+q)_\perp^2 - \frac{1-z_2^2}{4}(r_1-q)_\perp^2$$

The same result would emerge if we would have started with the lower vertex. Now we look at the contribution of the eikonal path, which in our language means that part of the x-integrations where $x_i \ll 1$. In this domain we approximate the integrand to:

$$I_{2a}=$$

$$\left(\frac{g^2}{2(2\pi)^3}\right)^2 \int d^2p_{1\perp} \int_0^{} dx_1 x_1^{\alpha(-(r_1+q)_\perp^2)} \int dp_{2\perp} \int_0^{\ll 1} dx_2 x_2^{\alpha(-(r_1-q)_\perp^2)} \tag{2.9}$$

$$\cdot \int dZ_1 dZ_2 \varrho(\vec{f}_1, z_1) \cdot \varrho(\vec{f}_2, z_2) \cdot \left(-\frac{i}{2}\right)^2 \int_0^\infty d\omega_1 \omega_1^2 d\omega_2 \omega_{2e}^2 - i\omega_1 D_{1e} - i\omega_2 D_{2e}$$

$$\cdot \theta\left(\omega_1 x_1 \frac{1+z_1}{2} - \omega_2 x_2 \frac{1+z_2}{2}\right) \cdot \theta\left(\omega_1 x_1 \frac{1-z_1}{2} - \omega_2 x_2 \frac{1-z_2}{2}\right)$$

In the same manner we calculate the impact factor due to Fig.2b:

$$I_{2b}=$$

$$\left(\frac{g^2}{2(2\pi)^3}\right)^2 \int d^2p_1 \; d^2p_2 \int_0^1 dx_1 \int_0^{1-x_1} dx_2 \frac{x_1^{\alpha(-(r_1+q)_\perp^2)} x_2^{\alpha(-(r_1-q)_\perp^2)}}{(1-x_1)(1-x_2)(1-x_1-x_2)}$$

$$\cdot \int dZ_1 dZ_2 \varrho(\vec{f}_1, z_1) \cdot \varrho(\vec{f}_2, z_2) \cdot \left(-\frac{i}{2}\right)^2 \int_0^\infty d\omega_1 \omega_1^2 d\omega_2 \omega_{2e}^2 - i\omega_1 D_{1e}^b - i\omega_2 D_{2e}^b \tag{2.10}$$

$$\cdot \theta\left(\omega_2 x_2 \frac{1+z_2}{2} - \omega_1 x_1 \frac{1+z_1}{2}\right) \cdot \theta\left(\omega_1 x_1 \frac{1-z_1}{2} - \omega_2 x_2 \frac{1-z_2}{2}\right)$$

with the notations

$$D_1^b = D_1 - x_1 \frac{1+z_1}{2}\left(\frac{(r_1+p_2+q)_\perp^2+m^2}{1-x_2} - \frac{(p_1+p_2+q)_\perp^2+m^2}{1-x_1-x_2}\right) - x_1 \frac{1-z_1}{2}\left(M^2 - \frac{(r_1-p_1-q)_\perp^2+m^2}{1-x_1}\right)$$

$$D_2^b = D_2 - x_2 \frac{1+z_2}{2}\left(M^2 - \frac{(r_1+p_2+q)_\perp^2+m^2}{1-x_2}\right) - x_2 \frac{1-z_2}{2}\left(\frac{(r_1-p_1-q)_\perp^2+m^2}{1-x_1} - \frac{(p_1+p_2+q)_\perp^2+m^2}{1-x_1-x_2}\right)$$

For small x_i this takes the same form as (2.9), except for the θ-functions. So we see the general scheme: when we limit ourselves to very small x_i, the expressions for the different structures of Fig.2a-d become equal up to θ-functions, which in an evident manner reflect the ordering of the reggeon's legs on the straight line. Summation of all these different orderings will then give the factorized form:

$$I_2 = I_{2a}+I_{2b}+I_{2c}+I_{2d}$$

$$=\left(\frac{g^2}{2(2\pi)^3}\right)^2 \int d^2p_1 \int_0^{\ll 1} dx_1 x_1^{\alpha(-(r_1+q)_\perp^2)} \int d^2p_2 \int_0^{\ll 1} dx_2 x_2^{\alpha(-(r_1-q)_\perp^2)}$$

$$\cdot \int dz_1 \frac{\varphi(\gamma_1,z_1)}{\left(\gamma_1+\frac{1+z_1}{2}(p_1-r_1)_\perp^2+\frac{1-z_1}{2}(p_1+q)_\perp^2-\frac{1-z_1^2}{4}(r_1+q)_\perp^2\right)^3} \tag{2.11}$$

$$\cdot \int dz_2 \frac{\varphi(\gamma_2,z_2)}{\left(\gamma_2+\frac{1+z_2}{2}(p_2+q)_\perp^2+\frac{1-z_2}{2}(p_2+r_1)_\perp^2-\frac{1-z_2^2}{4}(r_1-q)_\perp^2\right)^3}$$

$$= \tilde{b}(-(r_1+q)_\perp^2)\ \tilde{b}(-(r_1-q)_\perp^2)$$

where

$$\tilde{b}(-(r_1+q)_\perp^2)=\frac{g^2}{2(2\pi)^2}\int d^2p \int_0^{\ll 1} dx x^{\alpha(-(r_1+q)_\perp^2)} \frac{1}{(p_1-r_1)_\perp^2+m_r^2} \tag{2.12}$$

$$\cdot \frac{1}{(p_1+q)_\perp^2+m_r^2}\ b(-(p_1-r_1)_\perp^2,-(p_1+q)_\perp^2,-(r_1+q)_\perp^2)$$

The same structures contribute to the lower vertex, but then we must take into account the factor 1/2!, because of double counting. Our amplitude for the exchange of two reggeons containing all structures of Fig.2 at the upper and the lower vertex thus assumes the eikonal form:

$$T_2 = 2is\frac{(2\pi)^2}{2!}\left(\frac{-i}{2(2\pi)^2 s}\right)^2 \int d^2q\ \tilde{R}(s,-(r_1+q)_\perp^2)\ \tilde{R}(s,-(r_1-q)_\perp^2) \tag{2.13}$$

$$R(s,t) = \tilde{b}(t)\ s^{\alpha(t)}\ \xi(t)\ \tilde{b}(t) \tag{2.14}$$

The other possible orderings of the reggeons to the straight line such as Fig.3 are zero in our approximation. This reflects the well-known[17] fact that graphs with planar coupling between reggeons and external particles have no Regge cut and are of lower order in s than those with non-planar couplings. Therefore we have taken into account all dominant orderings.

III. Generalization to Multi-Regge-Exchange

The generalization to the exchange of n reggeons is now quite straightforward, and we shall give only the results and refer to Appendix A for details of the calculations. At first the question arises which vertex structures one has to take into account. In our approximation we find that only those structures are different from zero, in which - following the straight line from the incoming particle to the outgoing - all reggeons must be emitted first before any reggeon is again absorbed[+] (one counterexample is given in Fig. 4). That the other structures are zero in our formalism means that they are of lower order in energy, in analogy to the AFS-diagram for the two-reggeon-case. This result of ours is different from the results of Ref. 4, where all permutations of the reggeon's legs on the straight line are needed to get eikonalization, including the AFS-structure. Thus our formalism gives a more realistic insight into this problem than earlier studies.

Looking now at the "nested" graphs of Fig. 5, we find the same character as in the two-reggeon-case of Section II. The eikonal path is defined by $x_i = 0$, and when we take only the contributions of this path ($x_i \ll 1$), the only dependence on the permutations is contained in θ-functions, and the sum over all permutations makes then vanish. So in generalization of (2.13):

$$T_n = 2is\frac{1}{n!}\int d^2b\ e^{-2ir_{1\perp}b_\perp}\left(\frac{1}{2(2\pi)^2 s}\int d^2q\ e^{-iq_\perp b_\perp}\tilde{R}(s,-q_\perp^2)\right)^n \qquad (3.1)$$

Since $x_i \ll 1$ means that the large momenta are confined to the straight lines, the situation is very similar to the case of the generalized ladders [1].

Of course there is no justification in ϕ^3 to assume that only the regions $x_i \ll 1$ should contribute for large s. In fact one has to take into account the whole interval $0 < x_i < 1$. In order to suppress other x-values then $x_i \ll 1$,

[+] These structures we shall call "nested".

one would have to introduce a cutoff at the reggeon's coupling to the external particle, e.g.,

$$\theta\ (\varepsilon\omega - p_+) \tag{3.2}$$

for the upper vertex, where p is the momentum of the reggeon-leg and ε is a small positive constant. Of course, one would have to justify or to explain such form factors.

IV. Eikonalization in the weak-coupling limit

As we mentioned in the introduction there are several papers [4-8] in which eikonalization of regge-exchange is studied in another way: the regge-ladders are expanded in powers of the coupling constant g, then the highest power of $\ln s$ is found and these leading terms are summed up. In this approximation it was found that for two-reggeon exchange the Mandelstam diagram has the eikonal form in the high-energy limit, while for multi-Regge exchange one has to take the high-energy limit not of the full diagrams, but only of the eikonal-path contributions. On the other hand we found in our formalism that indeed the eikonal path gives the desired form of the amplitude, but there is no reason to divide the amplitude into distinct paths. We therefore want to show in this section what happens when we go to the approximation of Refs. 4-8. For getting this approximation we have to simply take explicitly ladders for the exchanged reggeons and make the limit $g \to 0$.

At first we need some properties of the spectral representation (2.4) and the trajectory function, which are derived by means of the Bethe-Salpeter Equation (details are found in Appendix B).

$$\alpha(t) \underset{g^2\to 0}{\sim} -1 + \frac{g^2}{16\pi^2}\int_0^1 dx \frac{1}{-x(1-x)t+m_r^2-i\varepsilon}$$
$$= -1 + \frac{g^2}{16\pi^2}\alpha_0(t) \tag{4.1}$$

$$\varrho(\zeta,z) \underset{g^2\to 0}{\to} ig \tag{4.2}$$

$$\varrho(\zeta,z) \sim \zeta^{-\alpha-1}\varrho_\infty(z), \quad \varrho_\infty(z) \underset{g\to 0}{\to} ig \tag{4.3}$$

With these functions we go back into (2.8) and perform the ω-integrations:

$$\left(\frac{g^2}{2(2\pi)^3}\right)^2 \int d^2p_{1\perp} d^2p_{2\perp} \int_0^1 dx_1 \int_0^{1-x_1} dx_2 \frac{x_1^{\alpha(-(r_1+q)_\perp^2)} x_2^{\alpha(-(r_1-q)_\perp^2)}}{(1-x_1)^2(1-x_1-x_2)} \tag{4.4}$$
$$\cdot \int dZ_1 dZ_2 \varrho(\zeta_1,z_1)\ \varrho(\zeta_2,z_2)\ \frac{1}{2^2}\frac{\partial^2}{\partial\zeta_1^2}\frac{\partial^2}{\partial\zeta_2^2}\left(\frac{1}{D_1^a}\cdot\frac{1}{\frac{x_2}{x_1}\mathrm{Max}\left(\frac{1+z_2}{1+z_1},\frac{1-z_2}{1-z_1}\right)D_1^a+D_2^a}\right)$$

Since with $g^2 \to 0$ the trajectory-function goes to -1 (4.1), there arise some divergences of the x-integrations at $x_i = 0$ and also at $x_i = 1$. At first we look at the point $x_1 = x_2 = 0$. We introduce other variables:

$$\tau_1 = x_1,\ \tau_2 = x_2/x_1: \quad dx_1 dx_2 x_1^{\alpha(-(r_1+q)_\perp^2)} x_2^{\alpha(-(r_1-q)_\perp^2)} \tag{4.5}$$
$$= d\tau_1 d\tau_2\, \tau_1^{\alpha(-(r_1+q)_\perp^2)+\alpha(-(r_1-q)_\perp^2)+1} \tau_2^{\alpha(-(r_1-q)^2)}$$

Using the asymptotic behavior of the spectral functions (4.3), we see that the integrand remains different from zero at $\tau_1 = \tau_2 = 0$:

$$\int dZ_1 dZ_2 \varrho(\zeta_1,z_1)\ \varrho(\zeta_2,z_2)\ \frac{1}{2^2}\frac{\partial^2}{\partial\zeta_1^2}\frac{\partial^2}{\partial\zeta_2^2}\left(\frac{1}{D_1^a}\cdot\frac{1}{\frac{x_2}{x_1}\mathrm{Max}\left(\frac{1+z_2}{1+z_1},\frac{1-z_2}{1-z_1}\right)D_1^a+D_2^a}\right) \tag{4.6}$$

$$\longrightarrow \int dZ_1 \frac{\varrho(\zeta_1,z_1)}{(D_1)^3} \int dZ_2 \frac{\varrho(\zeta_2,z_2)}{(D_2)^3}$$

Therefore both the τ_1-integration and the τ_2-integration diverge for $g^2 = 0$, and the coefficient of these divergencies, which is proportional to $1/g^4$, is found by partial integration of the τ-variables:

$$\frac{1}{g^4\,\alpha_o(-(r_1-q)_\perp^2)\;(\alpha_o(-(r_1+q)_\perp^2)+\alpha_o(-(r_1-q)_\perp^2))} \tag{4.7}$$

$$\cdot \lim_{g^2\to 0}\Big(\frac{g^2}{2(2\pi)^3}\int d^2p_{1\perp}\int dZ_1\frac{\varphi(\zeta_1,z_1)}{(D_1)^3}\cdot\frac{g^2}{2(2\pi)^3}\int d^2p_{2\perp}\int dZ_2\frac{\varphi(\zeta_2,z_2)}{(D_2)^3}$$

The remaining limits can be calculated with (4.1) - (4.3) and (B.15):

$$\lim_{g^2\to 0}\int d^2p_\perp\int dZ\frac{\varphi(\zeta,z)}{\left(\zeta+\frac{1+z}{2}(r_1+p)_\perp^2+\frac{1-z}{2}(p-q)_\perp^2\frac{1-z^2}{4}(r_1+q)_\perp^2\right)^3}$$

$$= ig\int d^2p\;\frac{1}{(r_1+p)_\perp^2+m_r^2}\;\frac{1}{(p-q)_\perp^2+m_r^2} \tag{4.8}$$

$$= 16\pi^2 ig\alpha_o(-(r_1+q)_\perp^2)$$

So the limit of the impact factor's contribution at $x_1 = x_2 = 0$ is:

$$I_{2a}\xrightarrow[g^2\to 0]{}(ig)^2\frac{\alpha_o(-(r_1+q)_\perp^2)}{\alpha_o(-(r_1+q)_\perp^2)+\alpha_o(-(r_1-q)_\perp^2)} \tag{4.9}$$

We could study the other divergent point, $x_1 = 1$, $x_2 = 0$, in a similar manner, but it is more convenient to utilize the fact that the vertices of Figs. 2a and 2c for ladders as reggeons are identical in their topology. Instead of investigation the path $x_1=1$, $x_2 = 0$ of Fig. 2a we can look at the eikonal path $x_1 = x_2 = 0$ of Fig. 2c, which differs from Fig. 2a only by the interchanged reggeons. So the result is (4.9) with $-q_\perp$ instead of $q_\perp$, and the sum of both is simply $(ig)^2$. As is well known [9], this is the square of the reggeon vertex function in the weak-coupling limit.

So we see that in the weak-coupling limit the momenta are forced to pass the diagram along definite paths, while in general the whole interval $0 < x_1 < 1$ contributes. Furthermore, since Figs. 2a and 2c are equivalent to the vertex of the Mandelstam diagram, we have found that for this diagram there are two such

paths, and for large energies the sum of these gives the eikonal approximation. This is, within our framework, the result of Refs. 4-8 and Ref. 10.

The study of Figs. 2b and 2d is postponed to the next section. Taking only the contributions of 2a and 2c we obtain for the two-reggeon exchange in the weak coupling limit:

$$T_2 = 2is\frac{(2\pi)^2}{2!}\left(\frac{-i}{2(2\pi)^2 s}\right)^2 \int d^2q (ig)^4 s^{\alpha(-(r_1+q)_\perp^2)+\alpha(-(r_1-q)_\perp^2)} \cdot \xi(-(r_1+q)_\perp^2)\cdot \xi(-(r_1-q)_\perp^2) \tag{4.10}$$

In generalizing to multi-Regge-exchange we confine ourselves for the moment to the structures of Fig. 7, which we call "maximal nested" in accordance with Ref. 6. Here we have the same mechanism as for the two-reggeon case (for details of these calculations see Appendix C). In the limit $g^2 = 0$ there are divergencies in the x-integrations, and those points of the x-integration at which the divergencies occur, define paths through the diagram. One of these paths is the eikonal path: $x_1 = \ldots = x_n = 0$ (for notations see Fig. 7, $p_{i+} = 2x_i$). When we take only these contributions and sum over all permutations of the reggeons, we get for the weak-coupling limit of the impact factors $(ig)^n$, which is precisely the n-th power of the reggeon-vertex function in the weak-coupling limit.

Finally we demonstrate in our formalism, why the eikonal approximation is not the true high-energy behavior in ϕ^3 for the exchange of more than two reggeons. To do this we have to look for other paths than the eikonal path. We take, for example, the maximal-nested graph for three reggeons (Fig. 7) and write down the analog of (2.10):

$$\left(\frac{g^2}{2(2\pi)^3}\right)^3 \prod_{i=1}^{3}\left(\int d^2p_{i\perp}\int_0^1 dx_i x^{\alpha_i}\int dZ_i\, \varrho(\xi_i, z_i)\ \frac{1}{2}\frac{\partial^2}{\partial\xi_i^2}\right) \cdot \frac{\theta(1-x_1)\theta(1-x_1-x_2)\theta(1-x_1-x_2-x_3)}{(1-x_1)^2(1-x_1-x_2)^2(1-x_1-x_2-x_3)} \cdot \frac{1}{D_1^m}\ \frac{1}{\frac{x_2}{x_1}M_{21}D_1^m+D_2^m}\ \frac{1}{\frac{x_3}{x_1}M_{32}M_{21}D_1^m+\frac{x_3}{x_2}M_{32}D_2^m+D_3^m} \tag{4.11}$$

$$M_{ik}=\mathrm{Max}\left(\frac{1+z_i}{1+z_k},\frac{1-z_i}{1-z_k}\right)$$

$$\alpha_1=\left(-(r_1+q_1)_\perp^2\right),\alpha_2=\left(-(q_2-q_1)_\perp^2\right),\alpha_3=\left(-(r_1-q_2)_\perp^2\right)$$

$$D_1^m=D_1-\frac{1+z_1}{2}x_1\left(M^2-\frac{p_{1\perp}^2+m^2}{1-x_1}\right)-\frac{1-z_1}{2}x_1\left(M^2-\frac{(r_1-p_1-q_1)_\perp^2+m^2}{1-x_1}\right)$$

$$D_2^m=D_2-\frac{1+z_2}{2}x_2\left(\frac{p_{1\perp}^2+m^2}{1-x_1}-\frac{(p_1+p_2+q_2)_\perp^2+m^2}{1-x_1-x_2}\right)-\frac{1-z_2}{2}\left(\frac{(r_1-p_1-q_1)_\perp^2+m^2}{1-x_1}-\frac{(r_1-p_1-p_2-q_1-q_2)_\perp^2+m^2}{1-x_1-x_2}\right) \tag{4.11}$$

$$D_3^m=D_3-\frac{1+z_3}{2}x_3\left(\frac{(p_1+p_2+q_2)_\perp^2+m^2}{1-x_1-x_2}-\frac{(p_1+p_2+p_3+q_1+q_2)_\perp^2+m^2}{1-x_1-x_2-x_3}\right)-\frac{1-z_3}{2}x_3\left(\frac{(r_1-p_1-p_2-q_1-q_2)_\perp^2+m^2}{1-x_1-x_2}-\frac{(p_1+p_2+p_3+q_1+q_2)_\perp^2+m^2}{1-x_1-x_2-x_3}\right)$$

$$D_1=\mathcal{J}_1+\frac{1+z_1}{2}(p_1-r_1)_\perp^2+\frac{1-z_1}{2}(p_1+q_1)_\perp^2-\frac{1-z_1^2}{4}(q_1+r_1)_\perp^2$$

$$D_2=\mathcal{J}_2+\frac{1+z_2}{2}(p_2+q_1)_\perp^2+\frac{1-z_2}{2}(p_2+q_2)_\perp^2-\frac{1-z_2^2}{4}(q_2-q_1)_\perp^2$$

$$D_3=\mathcal{J}_3+\frac{1+z_3}{2}(p_3+q_2)_\perp^2+\frac{1-z_3}{2}(p_3+r_1)_\perp^2-\frac{1-z_3^2}{4}(r_1-q_2)_\perp^2$$

Here we take the shortest path through the diagram via the legs of the first reggeon. This corresponds to the x-values $x_1=1$, $x_2 = x_3 = 0$. To study the divergencies at this point we introduce polar coordinates:

$$\bar{x}_1=1-x_1,\ \bar{x}_1=r\sin\vartheta\cos\varphi,\ x_2=r\sin\vartheta\sin\varphi,\ x_3=r\cos\vartheta$$

$$dx_1dx_2dx_3x_1^{\alpha_1}x_2^{\alpha_2}x_3^{\alpha_3} = drd\vartheta d\varphi r^{\alpha_2+\alpha_3+2}(\sin\vartheta)^{\alpha_2+1}(\cos\vartheta)^{\alpha_3}(\cos\varphi)^{\alpha_2}(1-r\sin\vartheta\cos\varphi)^{\alpha_1}$$

and find for the behavior of the integrand at r = 0:

$$\int dZ_1dZ_2dZ_3\,g(\varphi_1,z_1)g(\varphi_2,z_2)g(\varphi_3,z_3)\frac{1}{2^3}\frac{\partial^2}{\partial\varphi_1^2}\frac{\partial^2}{\partial\varphi_2^2}\frac{\partial^2}{\partial\varphi_3^2}$$

$$\cdot\left(\frac{1}{rD_1^m}\,\frac{1}{r\sin\vartheta\sin\varphi M_{21}D_1^m+D_2^m}\,\frac{1}{r\cos\vartheta M_{32}M_{21}D_1^m+\frac{ctg\vartheta}{\sin\varphi}M_{32}D_2^m+D_3^m}\right) \tag{4.12}$$

$$\sim\ r^{\alpha(-(r_1+q_1)_\perp^2)+2}$$

Therefore the integrand as a whole goes with $r \sim 0$ as:

$$\sim\ r^{\alpha(-(r_1+q_1)_\perp^2)+\alpha(-(q_2-q_1)_\perp^2)+\alpha(-(r_1-q_2)_\perp^2)} \tag{4.13}$$

So we see that the integral diverges as soon as the sum of the trajectories is -1. To understand this divergency we have to go back to the paragraph in Sec.II where we found the integration limit for the x-integrations (after 2.6). There we found that the integration of the "-"components in the upper vertex (which are then transformed to the y) gives zero if the x are outside the interval of $0 < x_i < 1$. More exactly the limits are not zero and one but const/ω and 1-const/ω. Up to now we could neglect these small corrections, but for the understanding of the divergency (4.13) it is important. The corrected integration limits have the effect that the s-behavior is not

$$s^{\alpha(-(r_1+q_1)^2)+\alpha(-(q_2-q_1)^2)+\alpha(-(r_1-q_2)_\perp^2)-2} \tag{4.14}$$

but s^{-3}. The behavior (4.14) holds only if one disregards the contributions of the shorter paths such as that due to $x_1 = 1$, $x_2 = x_3 = 0$. These paths dominate over the eikonal contribution in the high-energy limit; therefore the eikonal approximation cannot give the exact high-energy behavior in ϕ^3.

V. High-Energy Behavior of "Nested" Graphs

In this section we shall concentrate on the high energy behavior of different structures of the impact factors. As we found already in Section III independent upon the weak-coupling limit of the exchanged reggeons, only nested graphs as in Fig. 5 are dominant over the non-nested ones such as in Fig. 3 or 4.

At a first glance all nested graphs seem to be of the same order in s. But we found already in the last section that only a subset of the nested graphs, namely the "maximal nested" structures of Fig. 7, gave already the eikonal form in the weak-coupling limit, and it turns out that these maximal nested graphs are indeed the leading ones in the weak-coupling limit, and that there is a hierarchy of the other "nested" structures in their s-behavior.

At first we show this situation for the two-reggeon case. For the two maximal-nested structures in Figs. 2a and 2c we found that in the limit $g^2 = 0$ two integrations diverge proportional to $1/g^4$. We take now the expressions Fig. 2b, (2.10), and perform the integrations:

$$\text{const.}\int d^2p_{1\perp}d^2p_{2\perp}\int_0^1 dx_1\int_0^{1-x_1} dx_2 \frac{x_1^{\alpha(-(r_1+q)_\perp^2)}x_2^{\alpha(-(r_1-q)_\perp^2)}}{(1-x_1)(1-x_2)(1-x_1-x_2)}$$
$$\cdot\int dz_1dz_2 g(\gamma_1,z_1)g(\gamma_2,z_2)\frac{1}{2^2}\frac{\partial^2}{\partial\gamma_1^2}\frac{\partial^2}{\partial\gamma_2^2}\left(\frac{\frac{x_2}{x_1}\left(\frac{1+z_2}{1+z_1}-\frac{1-z_2}{1-z_1}\right)\theta\left(\frac{1+z_2}{1+z_1}-\frac{1-z_2}{1-z_1}\right)}{\left(\frac{x_2}{x_1}\frac{1+z_2}{1+z_1}D_1^b+D_2^b\right)\left(\frac{x_2}{x_1}\frac{1-z_2}{1-z_1}D_1^b+D_2^b\right)}\right) \tag{5.1}$$

There is only one point at which divergencies occur with $g^2 = 0$ and $\alpha \to -1$, namely the point $x_1 = x_2 = 0$. We introduce polar coordinates

$$dx_1 dx_2 x_1^{\alpha(-(r_1+q)_\perp^2)} x_2^{\alpha(-(r_1-q)_\perp^2)} = dr d\varphi r^{\alpha(-(r_1+q)_\perp^2)+\alpha(-(r_1-q)_\perp^2)} \cdot (\cos\varphi)^{\alpha(-(r_1+q)_\perp^2)} (\sin\varphi)^{\alpha(-(r_1-q)_\perp^2)} \qquad (5.2)$$

and see that only the r-integration diverges when $\alpha \to -1$, while the ϕ-integration does not diverge at $\phi = 0$ or $\frac{\pi}{2}$. So we have only one divergence proportional to $1/g^2$, which is the weak-coupling limit of the eikonal path. A similar situation holds for the structure of Fig. 2d.

The fact that cases 2b and 2d have less divergencies in $\frac{1}{g^2}$ and therefore as a whole higher power of g^2 than those of Figs. 2a and 2c is connected with the leading-lns behavior of graphs with structures of Fig. 2 at the upper and lower vertex. To see this, we take the trajectory-function in the approximation (4.1) and use that the impact factors are proportional to g^2 for Fig. 2a, 2c and g^4 in Fig. 2b, 2d. Then a two-Regge exchange diagram with structures 2a at the lower and the upper vertex has the power serie (from 2.5)):

$$s^{-3} \sum_m g^4 \frac{(g^2\alpha_o(-(r_1+q)_\perp^2)+g^2\alpha_o(-(r_1-q)_\perp^2))^m \ln s^m}{m!} \qquad (5.3)$$

while for a graph with structure 2a at the lower and 2b at the upper vertex we have:

$$s^{-3} \sum_m g^6 \frac{(g^2\alpha_o(-(r_1+q)_\perp^2)+g^2\alpha_o(-(r_1-q)_\perp^2))^m \ln s^m}{m!} \qquad (5.4)$$

Comparing terms with equal powers of g we find that graphs of the second type are lower than those of the first type by lns. This was already found in Ref.6,7.

This situation can be generalized to multi-Regge exchange. When we look at the numbers of divergent integrations proportional to $1/g^2$, we find a hierarchy. The most divergent and therefore leading, graphs are the maximal-nested graphs of Fig. 7. These are those graphs where the ordering of emission and absorption of the reggeons is the same, i.e. the reggeon emitted first is absorbed as the last and so on. To be more precise, we classify the ordering of the reggeon-legs to the straight line in the following way:

When the numbering of the exchanged reggeons is fixed (Fig.5), each diagram is characterized by the two permutations $(i_1, \ldots, i_n)$, $(j_1, \ldots, j_n)$ of the numbers $(1, \ldots, n)$. They define the ordering of emission and absorption. We classify these permutations according to Fig. 6: draw a ladder and denote the n points on the left-hand side by $i_1, \ldots, i_n$, on the right-hand side by $j_i, \ldots, j_n$. Then connect the points for which $i = j$ by rungs. In general there will be horizontal rungs, not crossed by any other, and some groups $G_1, \ldots, G_r$ of $l_1, \ldots, l_r$ rungs, respectively. These groups are defined such that they contain no horizontal, uncrossed rungs and that the i's on the one side are permutations of the j's on the other side (this means that no rung is leaving or entering the group). So the maximal-nested graphs have only horizontal, uncrossed rungs.

Now the statement, derived in Appendix C, is the following: the number of diverging x-integrations is

$$n-(l_1-1)-(l_2-1)-\ldots-(l_r-1)$$

and the leading power of g^2 in the limit $g^2 = 0$:

$$g^{n+2(l_1-1+l_2-1+\ldots+l_r-1)} \tag{5.5}$$

This result on powers of g is now transformed into a statement about powers of lns, such as in (5.3), (5.4): we showed that the minimal power of g for the impact factor is equivalent to the highest power lns for a term of the expansion on powers of the coupling constant. So we find that diagrams with maximal-nested structures and the upper and lower vertex will have the highest s-behavior. This was already suggested in Ref. 6, and we confirm it within our framework. Moreover, we have found that structures can be ordered in a hierarchy, according to their leading-lns behavior.

VI. Summary and Conclusions

What we have found is the following: starting from the general impact picture of Cheng and Wu - or, equivalently, from the form of the reggeon exchange amplitude that was used by Gribov and Winbow -, and taking a rather general ansatz for the reggeon amplitude, we have studied under what conditions we get the eikonal form for Regge exchange. In general the impact factors of the form of Fig. 5 are complicated expressions, namely multidimensional integrals over internal momenta, and they are far away from factorizing into a simple product of the reggeon vertexfunctions, as it would be necessary for eikonalization. In order to get the eikonal form one has to take from the full graphs of the form of Fig. 1 with impact factors of Fig. 5 at the upper and lower end only the contributions of the eikonal paths, i.e. those parts of the amplitudes where the large momenta pass the diagram along the straight lines at the upper and the lower end. Then one must sum over all permutations of the nested graphs (they are defined in III) and gets thus the eikonal form with slightly modified reggeon vertex functions. Thus the essential step in eikonalization of Regge exchange is the emission and absorption of very soft reggeons, while the momenta of the external particles remain essentially unchanged during the scattering process. This picture is quite analogous to the case of the exchange of virtual particles in the generalized ladder diagrams. But without the introduction of form factors it is not justified to take only the eikonal parts of the impact factors and to neglect the other parts.

This situation changes if one takes the weak coupling limit for the trajectory- and vertex functions of the exchanged reggeons. In this limit the impact factors decay into a sum of terms, each of which corresponds to a definite path of the large momentum through the diagram. One of these is the eikonal path. In ϕ^3, nevertheless, the eikonal parts are not the dominant ones for large s. There are always "shorter" paths with a higher s-power than the eikonal path. Only when one neglects all these shorter paths, then the eikonal form emerges. But this concerns only the weak coupling limit of the exchanged reggeons.

In order to achieve eikonalization independently on the weak coupling limit of the exchanged reggeons, one has to modify the coupling of the reggeons to the external particles by the introduction of form factors. So it could be a future task to study within our framework the effect of such form factors.

Apart from this detailed study of the mechanism of eikonalization we have looked which structures of the reggeon couplings to the external particles do contribute. We found that certain structures of multi-Regge exchange, such as the AFS-structure for double Regge exchange, are not at all important at high energies. Only those structures which we called "nested" do contribute. Moreover, in the weak coupling limit these "nested" graphs are not all of the same order. They can be put into a hierarchy according to their high-energy behavior, and the leading ones are the "maximal-nested". This was already supposed in Ref.6.

In conclusion we would like to make a remark about the limitations of our technique. Our steps of approximation in writing down the expressions for the impact factors can be justified either by the experience of Cheng and Wu or by appropriate damping properties of the reggeon-amplitudes for large values of the external masses and momentum transfer. More rigorous methods, such as an investigation of Feynman-parameter representations, are not applicable for our aim, because they do not allow to take into account more than leading orders of lns in the expressions for the reggeons, nor are they simple enough to study more than double-Regge exchange. On the other hand our results fit very well into those of more rigorous investigations.

Of course we have been able to study only the leading-s-coefficient for the individual impact factors, and when we sum over all numbers of exchanged reggeons, we actually sum again only over leading s-terms, which must not be the high-energy limit of the sum. But in this respect the situation is very similar to that in potential scattering. There it is known [17] that in the Born expansion of the scattering amplitude each term for large s has the form of the corresponding part of the eikonal expansion. Thus the eikonal approximation is also the sum of leading terms of the Born expansion. In our case the reggeon represents the "potential", and the Born expansion in potential scattering corresponds to the expansion in numbers of exchanged reggeons in our case. Since we have taken the reggeons not in a weak-coupling limit but their full amplitude we have found the leading s-term for each number of exchanged reggeons, and so we have reached a level of rigorousness similar to that in potential scattering.

The author wants to thank Prof. G. Kramer for helpful discussions .

Appendix A

This Appendix contains calculations of Section III, i.e. the generalization of the eikonalization procedure to the multi-Reggeon-dase. Our notation of the momenta is given in Fig. 5: when the reggeons are numbered 1, ...n, then each individual diagram is characterized by the two permutations $i_1, \ldots, i_n$, $j_1, \ldots j_n$, which define the ordering of emission and absorption of the reggeons by the line of the external particle. Equivalently we use permutations $\mu_1, \ldots, \mu_n$ and $\nu_1, \ldots \nu_n$, where μ_k is the number of the vertex where the reggeon k is emitted, and ν_k the number of the vertex where it is absorbed (for the emission we have counted from the left, for absorption from the right). Now we introduce some new variables:

$$(p_k)_+ = 2x_k\omega, \quad 2\omega(p_k)_- = y_k, \quad 2\omega(q_{ij})_- = y_{ij} \tag{A.1}$$
$$y_k + k_{kk-1} = \alpha_k, \quad y_k + y_{kk+1} = \beta_k$$

and have for the denominators along the straight line from the left to the right:

$$\begin{aligned}
&(1-x_{i_1})(M^2-\varphi_1)-F_1+i\varepsilon \\
&(1-x_{i_1}-x_{i_2})(M^2-\varphi_2)-F_2+i\varepsilon \\
&\ldots \\
&(1-x_{i_1}-\ldots-x_{i_{n-1}})(M^2-\varphi_{n-1})-F_{n-1}+i\varepsilon \\
&(1-x_1-\ldots x_n)(M^2-\lambda)-K+i\varepsilon \\
&(1-x_{j_1}-\ldots-x_{j_{n-1}})(M^2-\psi_{n-1})-L_{n-1}+i\varepsilon \\
&\ldots \\
&(1-x_{j_1})(M^2-\psi_1)-L_1+i\varepsilon
\end{aligned} \tag{A.2}$$

$$F_k = (r_1 + p_{i_1} + q_{i_1 i_1 - 1} + \ldots + p_{i_k} + q_{i_k i_k - 1})_\perp^2 + m^2$$
$$L_k = (-r_1 + p_{j_1} + q_{j_1 j_1 + 1} + \ldots + p_{j_k} + q_{j_k j_k + 1})_\perp^2 + m^2$$
$$K = (p_1 + q_{10} + \ldots + p_n + q_{nn-1})_\perp^2 + m^2 = (p_1 + q_{12} + \ldots + p_n + q_{nn+1})_\perp^2 + m^2$$

$$\varphi_k=\alpha_{i_1}+\ldots+\alpha_{i_k}\ ,\ \psi_k=\beta_{j_1}+\ldots+\beta_{j_k}\ ,\quad \lambda=\sum_1^n\alpha_k=\sum_1^n\beta_k \tag{A.2}$$
$$\alpha_k=\varphi_{\mu_k}-\varphi_{\mu_k-1}\ ,\quad \beta_k=\psi_{\nu_k}-\psi_{\nu_k-1}\quad(\varphi_n=\psi_n=\lambda,\ \varphi_o=\psi_o=0)$$

Similarly the denominators of the spectral forms for the reggeons:

$$D_k=\mathcal{J}_k-\frac{1+z_k}{2}(x_k\alpha_k-(p_k+q_{kk+1})_\perp^2)-\frac{1-z_k}{2}(x_k\beta_k-(p_k+q_{kk+1})_\perp^2)$$
$$-\frac{1-z_k}{4}(q_{kk-1}-q_{kk+1})_\perp^2-i\varepsilon \tag{A.3}$$
$$=\mathcal{J}_k+\frac{1+z_k}{2}(p_k+q_{kk-1})_\perp^2-\frac{1-z_k}{2}(p_k+q_{kk+1})_\perp^2-\frac{1-z_k^2}{4}(q_{kk-1}-q_{kk+1})_\perp^2$$
$$-\frac{1+z_k}{2}x_k(\varphi_{\mu_k}-\varphi_{\mu_k-1})-\frac{1-z_k}{2}x_k(\psi_{\nu_k}-\psi_{\nu_k-1})-i\varepsilon$$

We use now the expression (2.7) for the reggeon denominators, perform the integration of the λ,φ,ψ and have in analogy to (2.8):

$$\left(\frac{g^2}{2(2\pi)^3}\right)^n\ \prod_{k=1}^n\Big(\int d^2p_{k\perp}\int dx_k x_k^{\alpha}\,(-(q_{kk+1}-q_{kk-1})_\perp^2)\int dz_k\,\varrho(\mathcal{J}_k,z_k)$$
$$-\frac{i}{2}\int_o^\infty d\omega_k\omega_k^2\ e^{-i\omega_k D_k}\Big) \tag{A.4}$$
$$\cdot\frac{\mathrm{sgn}(X_{i_1})}{X_{i_1}}\,\frac{\mathrm{sgn}(X_{i_2})}{X_{i_2}}\ldots\frac{\mathrm{sgn}(X_{i_{n-1}})}{X_{i_{n-1}}}\,\frac{\mathrm{sgn}(X_n)}{X_n}\,\frac{\mathrm{sgn}(X_{j_{n-1}})}{X_{j_{n-1}}}\ldots\frac{\mathrm{sgn}(X_{j_1})}{X_{j_1}}$$
$$\cdot\theta\Big(\frac{\omega_{i_1}^+x_{i_1}-\omega_{i_2}^+x_{i_2}}{X_{i_1}}\Big)\cdot\theta\Big(\frac{\omega_{i_2}^+x_{i_2}-\omega_{i_3}^+x_{i_3}}{X_{i_2}}\Big)\ldots\theta\Big(\frac{\omega_{i_{n-1}}^+x_{i_{n-1}}-\omega_{i_n}^+x_{i_n}}{X_{i_{n-1}}}\Big)$$
$$\cdot\theta\Big(\frac{\omega_{j_1}^-x_{j_1}-\omega_{j_2}^-x_{j_2}}{X_{j_1}}\Big)\cdot\theta\Big(\frac{\omega_{j_2}^-x_{j_2}-\omega_{j_3}^-x_{j_3}}{X_{j_2}}\Big)\ldots\theta\Big(\frac{\omega_{j_{n-1}}^-x_{j_{n-1}}-\omega_{j_n}^-x_{j_n}}{X_{j_{n-1}}}\Big)$$

with the abbreviations:

$$X_{i_k} = 1 - x_{i_1} - \ldots - x_{i_k}$$

$$X_{j_k} = 1 - x_{j_1} - \ldots - x_{j_k} \qquad \omega_k^{\pm} = \omega_k \frac{1 \pm z_k}{2}$$

$$X_n = 1 - x_1 - \ldots - x_n$$

A detailed study of the θ-functions shows that the ω-integrations are different from zero only, when all $x_k > 0$ and $X_k > 0$. So one can neglect all the denominators of the arguments of the θ-functions because they are positive, and because the sgn-functions are all +1. Now we confine ourselves to the eikonal path (x_i nearly zero) and set $x_i = 0$ everywhere in the integral with the exception of the θ-functions and the x^{α}-factors. The dependence on the individual permutations we get the eikonal form (see (2.11)):

$$\left(\frac{g^2}{2(2\ )^3}\right)^n \prod_{k=1}^{n} \Big(\int d_2 p_{k\perp} \int_0^{\ll 1} dx_k x_k^{\alpha(-(q_{kk+1}-q_{kk-1})_\perp^2)} \int dz_k \varrho(\gamma_k, z_k) \cdot -\frac{i}{2} \int_0^{\infty} d\omega_k \omega_k^2 \, e^{-i\omega_k D_k} \Big)$$

$$= \prod_{k=1}^{n} \Big(\left(\frac{g^2}{2(2\ )^3}\right) \int d^2 p_{k\perp} \frac{b(-(p_k+q_{kk-1})_\perp^2, -(p_k+q_{kk+1})_\perp^2, -(q_{kk-1}-q_{kk+1})_\perp^2)}{((p_k+q_{kk-1})^2+m^2)\ ((p_k+q_{kk+1})^2+m^2)} \cdot \int_0^{\ll 1} dx_k x_k^{\alpha(-(q_{kk+1}-q_{kk-1})_\perp^2)} \Big) \qquad (A.5)$$

$$= \prod_{k=1}^{n} \tilde{b}(-(q_{kk-1}-q_{kk+1})_\perp^2)$$

Up to now we have considered only the "nested" graphs, those in which at first all reggeons are emitted in an arbitrary order and then again absorbed. If we now take a non-nested graph as in Fig. 4, then by proceeding in the same way as in (A.4) we get again a series of θ-functions. But these θ-functions are incompatible, and there are no x-intervals for which the ω-integrations are different from zero. So in our approximation these graphs do not contribute, which means that they are of lower s-dependence.

Appendix B

We shall derive some properties of the spectral representations (2.3), (2.4) for the case that the reggeons are ϕ^3-ladders. We follow the procedure of Ref. 10 and use again infinite-momentum techniques, as we have already done in the calculations for the impact factors. We expect our results to be valid only in the weak coupling limit, but that is all we are interested in for the moment. We write down the Bethe-Salpeter-Equation for the ladder approximation (Fig.8), use the spectral ansatz (2.3) and decompose the denominators according to Ref. 15 in the following form:

$$\frac{1}{(r_2-p)^2-\mu^2}\;\frac{1}{\gamma'-\frac{1+z'}{2}(p-r_1)^2-\frac{1-z'}{2}(p+r_1)^2+\frac{1-z'^2}{4}(2r_1)^2}$$

$$\frac{1}{(p-r_1)^2-m_r^2}\;\frac{1}{(p+r_1)^2-m_r^2} \tag{B.1}$$

$$=\frac{1}{(r_2-p)^2-\mu^2}\;\frac{1}{\gamma'-\frac{1+z'}{2}(p-r_1)^2-\frac{1-z'}{2}(p+r_1)^2+\frac{1-z'^2}{4}(2r_1)^2}$$

$$\left(\frac{1}{(p-r_1)^2-m_r^2}\;\frac{1}{(p+r_1)^2-m_r^2}+\left(\frac{\frac{1+z'}{2}}{(p-r_1)^2-m_r^2}+\frac{\frac{1-z'}{2}}{(p+r_1)^2-m_r^2}\right)\right.$$

$$\left.\frac{1}{\gamma'-\frac{1+z'}{2}(p-r_1)^2-\frac{1-z'}{2}(p+r_1)^2+\frac{1-z'^2}{4}(2r_1)^2}\right)$$

Now we use the same approximations as in the derivation of the impact factors, perform the p_- and p_+-integrations by taking the residues and by symmetrical integration, respectively, and get for the spectral-function the integral equation:

$$\bar{g}(\gamma,z)=\frac{g^2}{8(2\pi)^2}\int_{-1}^{+1}dz'\int_{\gamma_0(z')}^{\infty}d\gamma'\;K(\gamma,z;\gamma',z')\cdot\bar{g}(\gamma',z') \tag{B.2}$$

where we have used the following abbreviations:

$$K(\gamma,z;\gamma',z')=\int_0^1 dx\,x^{\alpha((2r_1)^2)-1}\,\frac{\delta\left(\frac{M(z)^2}{x}-\frac{\mu^2}{1-x}\right)-\delta\left(\frac{\tilde{M}(z)^2}{x}-\frac{\mu^2}{1-x}\right)}{\gamma'-M(z')^2} \tag{B.3}$$

$$M(z)^2 = \frac{1+z}{2} m_r^2 + \frac{1-z}{2} m_r^2 - \frac{1-z^2}{4}(2r_1)^2 \tag{B.4}$$

$$\tilde{M}(z)^2 = \begin{cases} \dfrac{\frac{1+z}{2}\left(\varsigma' - \frac{1-z'}{2} m_r^2 + \frac{1-z'^2}{4}(2r_1)^2\right)}{\frac{1+z'}{2}} + \frac{1-z}{2} m_r^2 - \frac{1-z^2}{4}(2r_1)^2 & z<z' \\ \dfrac{\frac{1+z}{2} m_r^2 + \frac{1-z}{2}\left(\varsigma' - \frac{1+z'}{2} m_r^2 + \frac{1-z'^2}{4}(2r_1)^2\right)}{\frac{1-z'}{2}} - \frac{1-z^2}{4}(2r_1)^2 & z>z' \end{cases} \tag{B.5}$$

$$\tilde{\varsigma}_0(z) = (M(z)+\mu)^2 \tag{B.6}$$

At first we look at the large-ρ-behavior: after performing the x-integration by means of the δ-functions we find the form:

$$K(\varsigma, z; \varsigma', z') \underset{\varsigma \to \infty}{\sim} \varsigma^{-\alpha(t)-1} \frac{(M(z)^2)^{\alpha(t)} - (\tilde{M}(z)^2)^{\alpha(t)}}{\varsigma' - M(z')^2} \tag{B.7}$$

$$\bar{\rho}(\varsigma, z) \underset{\varsigma \to \infty}{\sim} \varsigma^{-\alpha(t)-1} \bar{g}_\infty(z) \tag{B.8}$$

$$\bar{g}_\infty(z) = \frac{g^2}{8(2\pi)^2} \int_{-1}^{+1} dz' \int_{\varsigma_0(z')}^{\infty} d\varsigma' \, \frac{(M(z)^2)^{\alpha(t)} - (\tilde{M}(z)^2)^{\alpha(t)}}{\varsigma' - M(z')^2} \bar{\rho}(\varsigma', z') \tag{B.9}$$

Now we take the limit $g^2 \to 0$. In order to have the same power of g^2 on both sides of (B.9), there must be one divergent integration in the limit $g^2 = 0$ which cancels the factor g^2 in front of the integral. Such a divergence arises for

$$\alpha(t) \underset{g^2 \to 0}{\to} -1 + \frac{g^2}{16\pi^2} \alpha_0(t) \tag{B.10}$$

where $\alpha_0(t)$ has to be determined by the equation. For $\alpha \sim -1$ we may neglect the second term in (B.9) because of the ρ'-dependence in $\tilde{M}(z)^2$ and get in the limit $\alpha \to -1$:

$$\bar{\varrho}_\infty(z) = \frac{g^2}{8(2\pi)^2}\ \frac{1}{M(z)^2}\ \frac{16\pi^2}{g^2\alpha_0(t)} \int_{-1}^{+1} dz'\,\bar{\varrho}_\infty(z') \tag{B.11}$$

Integrating both sides with respect to z, we have:

$$\alpha_0(t) = \int_0^1 dx\ \frac{1}{(-x(1-x)t+m_r^2)} \tag{B.12}$$

in accordance with perturbational calculations[20]. But there is still one unknown constant, an overall factor of $\bar{\rho}^\infty$, which cannot be determined by means of our homogeneous integral equation. This constant can be found, since we know the limit of the vertex function for small g^2: it must be ig [20]: This gives:

$$ig = \lim_{g^2\to 0} \int_{-1}^{+1} dz \int_{\bar{\varphi}_0(z)}^{\infty} d\varphi\ \frac{\varrho(\varphi,z)}{\varphi - \frac{1+z}{2}m_r^2 - \frac{1-z}{2}m_r^2 + \frac{1-z^2}{4}t} \tag{B.13}$$

$$= \frac{16\pi^2}{g^2\alpha_0(t)} \int_{-1}^{+1} dz'\ \lim_{g^2\to 0}\bar{\varrho}_\infty(z')$$

(B.14)

$$\lim_{g^2\to 0}\bar{\varrho}_\infty(z) = \frac{ig^3}{8(2\pi)^2}\ \frac{1}{M(z)^2}$$

Next we are interested in the represenation (2.4):

$$\frac{1}{k_1^2-m_r^2}\ \frac{1}{k_2^2-m_r^2} \int_{-1}^{+1} dz \int_{\bar{\varphi}_0(z)}^{\infty} d\varphi\ \frac{\bar{\varrho}(\varphi,z)}{\varphi - \frac{1+z}{2}\ k_1^2 - \frac{1-z}{2}\ k_2^2 + \frac{1-z^2}{4}t} \tag{B.15}$$

We combine the denominators by means of the Feynman identity and introduce new variables with δ-functions:

$$= \int_{-1}^{+1} dz \int_{\varphi_0(z)}^{\infty} d\ \frac{\varrho(\varphi,z)}{(\varphi - \frac{1+z}{2}k_1^2 - \frac{1-z}{2}k_2^2 + \frac{1-z^2}{4}t)^3} \tag{B.16}$$

$$\varphi_0(z) = M(z)^2 = m_r^2 - \frac{1-z^2}{4}t \tag{B.17}$$

where the new spectral function is connected with the other one by:

$$\varrho(\zeta,z)=\int_0^1 dy\frac{1}{y}\int_{\mathrm{Max}(\frac{z-(1-y)}{y},\,-1)}^{\mathrm{Min}(\frac{z+(1-y)}{y},\,1)} dz'\bar{\varrho}\left(\frac{\zeta-m_r^2+\frac{1-z^2}{4}t}{y}+m_r^2-\frac{1-z'^2}{4}t,z'\right)\cdot\Theta\left(\frac{\zeta-m_r^2+\frac{1-z^2}{4}t}{y}+M(z')^2-(M(z')+\mu)^2\right) \tag{B.18}$$

Finally the following properties are important:

$$\varrho(\zeta,z)\underset{\zeta\to\infty}{\sim}\zeta^{-\alpha(t)-1}\varrho_\infty(z) \tag{B.19}$$

$$\varrho_\infty(z)\xrightarrow[g^2\to 0]{} \text{ig}$$

Appendix C

In the following we give some more details of the weak-coupling limit for n reggeon exchange. At first we shall consider the maximal-nested diagrams of Fig. 7, then we show how the maximal-nested graphs dominate over the other structures.

We take (A.4) for the case that $(i_1,\ldots,i_n) = (j_1,\ldots,j_n)$, and perform the ω-integrations:

$$\left(\frac{g^2}{2(2\pi)^3}\right)^n \prod_{k=1}^{n} \left(\int d^2p_{k\perp} \int_{>0} dx_k x_k^{\alpha(-(q_{kk+1}-q_{kk-1})_\perp^2)} \int dz_k \varphi(\gamma_k, z_k) \frac{1}{2}\frac{\partial^2}{\partial \gamma_k^2} \right)$$

$$\cdot \frac{\theta(x_{i_1})}{x_{i_1}^2} \frac{\theta(x_{i_2})}{x_{i_2}^2} \cdots \frac{\theta(x_n)}{x_n} \qquad \text{(C.1)}$$

$$\cdot \frac{1}{D_{i_1}} \frac{1}{\frac{x_{i_2}}{x_{i_1}} M_{i_2 i_1} D_{i_1} + D_{i_2}} \cdots \frac{1}{\frac{x_{i_n}}{x_{i_1}} M_{i_n i_{n-1}} \cdots M_{i_2 i_1} D_{i_1} + \ldots + D_{i_n}}$$

To study the eikonal path ($x_1 = \ldots = x_n = 0$) we find it convenient to introduce other variables:

$$\tau_1 = x_{i_1}, \quad \tau_2 = \frac{x_{i_2}}{x_{i_1}}, \quad \ldots, \quad \tau_n = \frac{x_{i_n}}{x_{i_{n-1}}} \qquad \text{(C.2)}$$

$$dx_{i_1} \ldots dx_{i_n} x_{i_1}^{\alpha_{i_1}} \ldots x_{i_n}^{\alpha_{i_n}} = d\tau_1 \ldots d\tau_n \tau_1^{n-1+\alpha_{i_1}+\ldots+\alpha_{i_n}} \ldots \tau_n$$

Using the asymptotic-ρ-behavior of the spectral function (B.19), we see that in the limit $\tau_1 = \ldots = \tau_n = 0$ the integrand has the form:

$$\frac{1}{(D_{i_1})^3 \ldots (D_{i_n})^3} \qquad \text{(C.3)}$$

This has the consequence that in the limit $g^2 = 0$ all τ-integrations diverge proportional to $1/g^{2n}$. The coefficient of this leading divergent term is found by partial integration of the τ's and contains a factor of the form:

$$\frac{1}{\alpha_{oi_1}+\ldots+\alpha_{oi_n}}\;\frac{1}{\alpha_{oi_2}+\ldots+\alpha_{oi_n}}\;\cdots\;\frac{1}{\alpha_{oi_n}} \tag{C.4}$$

The rest is independent of the individual permutation. Thus the sum over all permutations gives $(ig)^n$.

Now we take an arbitrary non-maximal-nested graph. If we would try to perform the ω-integrations in (A.4), we would get a very complicated expression. So we make a simplification of the spectral form (II.4) which facilates our calculations. In the foregoing study of the weak-coupling limit we saw that we needed the asymptotic-ρ-behavior (B.19) together with its coefficient in the limit $g^2 = 0$. In particular the z-dependence of the asymptotic form dropped out. Therefore we are allowed to use the simplified form:

$$\int_{-1}^{+1} dz \int_{\varsigma_0(z)}^{\infty} d\varsigma \;\frac{\sigma(\varsigma)}{\left(\varsigma-\frac{1+z}{2}p_1^2-\frac{1-z}{2}p_1'^2+\frac{1-z^2}{4}t\right)^3}\;, \qquad \sigma(\varsigma)\underset{\varsigma\to\infty}{\sim} ig\varsigma^{-\alpha(t)-1} \tag{C.5}$$

This can be cast into the form:

$$\int_{m^2}^{\infty} d\varsigma \frac{\left(\delta(\varsigma-m_r^2)+\frac{\partial}{\partial\varsigma}\right)\sigma(\varsigma)}{(\varsigma-p_1^2)\;(\varsigma-p_1'^2)}$$

$$=\int_{m^2}^{\infty} d\varsigma \frac{\sigma_0(\varsigma)}{(\varsigma-p_1^2)\;(\varsigma-p_1'^2)}\;,\; \sigma_0(\varsigma)\underset{\varsigma\to\infty}{\sim} ig^3\varsigma^{-\alpha(t)-2}\cdot \text{Function}(t) \tag{C.6}$$

With this ansatz we write down once more the expression for the general nested diagram. The denominators along the straight line are the same as in (A.2), while those of the reggeon legs are:

$$x_k\alpha_k - r_k \qquad \text{and} \qquad x_k\beta_k - s_k$$

with

$$r_k=(p_k+q_{kk-1})_\perp^2+\varsigma_k$$
$$s_k=(p_k+q_{kk+1})_\perp^2+\varsigma_k$$

After performing the α,β-integrations we have the following denominators:

$$\frac{1-x_1-\ldots-x_n}{(x_1\ldots x_n)^2}\;\frac{1}{(1-x_{i_1})(M^2-\frac{r_{i_1}}{x_{i_1}})-F_1}\cdots\frac{1}{(1-x_{i_1}-\ldots-x_{i_n})(M^2-\frac{r_{i_1}}{x_{i_1}}-\ldots-\frac{r_{i_n}}{x_{i_n}})-K} \tag{C.7}$$

$$\cdot\;\frac{1}{(1-x_{j_1})(M^2-\frac{s_{j_1}}{x_{j_1}})-L_1}\cdots\frac{1}{(1-x_{j_1}-\ldots-x_{j_n})(M^2-\frac{s_{j_1}}{x_{j_1}}-\ldots-\frac{s_{j_n}}{x_{j_n}})-K}$$

Since we are interested in the limit for very small x, we may already make some simplifications:

$$\frac{1}{r_{i_1}}\;\frac{1}{\frac{x_{i_2}}{x_{i_1}}r_{i_1}+r_{i_2}}\cdots\frac{1}{\frac{x_{i_n}}{x_{i_1}}r_{i_1}+\frac{x_{i_n}}{x_{i_2}}r_{i_2}+\ldots+r_{i_n}} \tag{C.8}$$

$$\cdot\;\frac{1}{s_{j_1}}\;\frac{1}{\frac{x_{j_2}}{x_{j_1}}s_{j_1}+s_{j_2}}\cdots\frac{1}{\frac{x_{j_n}}{x_{j_1}}s_{j_1}+\frac{x_{j_n}}{x_{j_2}}s_{j_2}+\ldots+s_{j_n}}$$

Now the dominance of the maximal-nested graphs over the other structures is due to the following reasons. In the limit $g^2 = 0$ the trajectory-function goes to -1, and all x-integrations would diverge at 0, if the other integrand would not vanish. Then we would get a factor $1/g^{2n}$ as in the case of the maximal-nested graphs.

For that case we introduced the τ-variables and found the limit (C.3). This situation now becomes clearer in (C.8). For the maximal nested case $i_1 = j_1,\ldots, i_n = j_n$, and after the introduction of the -variables, only occur the denominator continues only products of τ's but no quotients, but there are no quotients of τ's. Therefore the limit $\tau \to 0$ can be taken for all τ independently, and the denominators remain all different from zero. This situation changes if there are some i's unequal to some j's: e.g. $i_1 = j_2$, $i_2 = j_1$ and $i_k = j_k (k=3,\ldots,n)$. Then there are both

$$x_{i_2}/x_{i_1} \quad \text{and} \quad x_{j_2}/x_{j_1} = x_{i_1}/x_{i_2}$$

in the denominators and if x_{i_1} or x_{i_2} go to zero in such a way that one of the

ratios $\to 0$ too, then we have an infinity in the denominator, and the whole expression is zero. So only $x_{i_1} \sim x_{i_2} \to 0$ with fixed ratio are possible:

$$x_{i_1} = r \cos\varphi, \qquad x_{i_2} = r \sin\varphi$$

and only the limit $r \to 0$ gives a divergence for $g^2 = 0$, while $\phi = 0$ or $\phi = \frac{\pi}{2}$ do not give divergences. For the other x we again introduce τ-variables as (C.2) and get n-2-divergent integrations. So we have a total of n-1-divergent integrations, and n for the maximal-nested graphs.

This can be generalized. According to the prescription of Section V we draw the ladder of Fig. 6 and devide the graphs into groups: the horizontal, uncrossed ones and the groups of the other type described. Then we find that for the groups G_k we should introduce polar coordinates for the x_i with radii r_k, and these r_k give one divergent integration, respectively. The corresponding angles have no effect in the limit $g^2 = 0$. The x-variables of the free, uncrossed rungs can be treated as in the maximal-nested case, i.e. the can be transformed into τ's. Each such τ gives an additional divergence. So on the whole we have

$$n-(l_1-1)-(l_2-1)-\ldots-(l_r-1) \tag{C.9}$$

divergent integrations, and the resulting powers of g in the weak-coupling limit for one impact factor are

$$g^{n+2(l_1-1+l_2-1+\ldots+l_r-1)} \tag{C.10}$$

References

1. G.Tictopoulos and S.B.Treiman: Phys.Rev. D 2, 805 (70) and Phys.Rev. D 3, 1037 (70).
2. H.Cheng and T.T.Wu: Phys.Rev. 186, 1611(69) and Phys.Rev. D 1(2775), Phys.Rev. D1, 2775(70).
3. S.-J.Chang and P.M.Fishbane: Phys.Rev. D 2, 1104(70).
4. S.-J.Chang and P.M.Fishbane: Phys.Rev. D 4, 537 (71).
5. B.Hasslacher, D.K.Sinclair, G.M.Cicuta and R.L.Sugar: Phys.Rev.Let.25, 1591 (70).
6. B. Hasslacher and D.K.Sinclair: Phys.Rev. D 3, 1770 (71).
7. G.M.Cicuta and R.L.Sugar: Phys.Rev. D 3, 970 (71).
8. A.R.Swift: Phys.Rev. D 5, 1400 (72).
9. R.J.Eden, P.V.Landshoff, D.I.Olive and J.C.Polkingborne: Cambridge Press 1966, The Analytic S-Matrix.
10. H.Cheng and T.T.Wu: Phys.Let. 34 B, 647 (71) and DESY 71/13 and DESY 71/16.
11. H.Cheng and T.T.Wu: Phys.Rev.Let. 24, 1456 (70).
12. H.Cheng and T.T.Wu: for ϕ^3 see Ref. 10, for QED e.g. Phys.Rev.Let.22,666(69).
13. V.N.Gribov: JETP 53, 654(67).
14. G. Winbow: Phys.Rev. 177, 2533(69).
15. G.Kramer and K.Meetz: Comm.Math.Phys. 3, 29(66).
16. N.Nakanishi: Phys.Rev. 130,1230(63) and Phys.Rev.133,B 1224(64).
17. H.Rothe: Phys.Rev. 159, 1471(67).
18. P.D.B.Collins: Springer Tracts in Modern Physics, Berlin-Heidelberg-New York, Vol. 60, p.204.
19. W.Hunziker: Helv.Phys.Acta 36, 838(63),
    L.I.Schiff: Phys.Rev. 103,443(56),
    T.T.Wu: Phys.Rev. 108,446(57).
20. J.C.Polkingborne: Journ.Math.Phys.4, 503(63),
    T.L.Trueman and T.Yao: Phys.Rev.132, 274(63),
    P.G.Federbush and M.T.Grisaru: Ann.Phys.22, 263(63),
    B.W.Lee and R.F.Sawyer: Phys.Rev. 127, 2266(62).

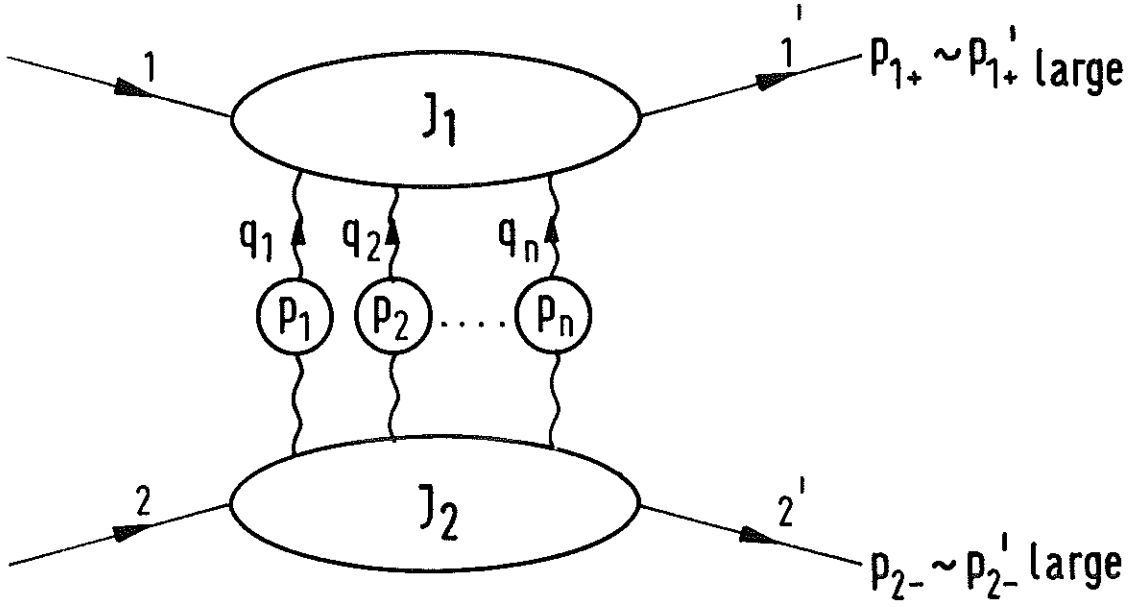
1
1'
$p_{1+} \sim p_{1+}'$ large
J_1
q_1
q_2
q_n
p_1
p_2
p_n
2
2'
J_2
$p_{2-} \sim p_{2-}'$ large

Fig.1

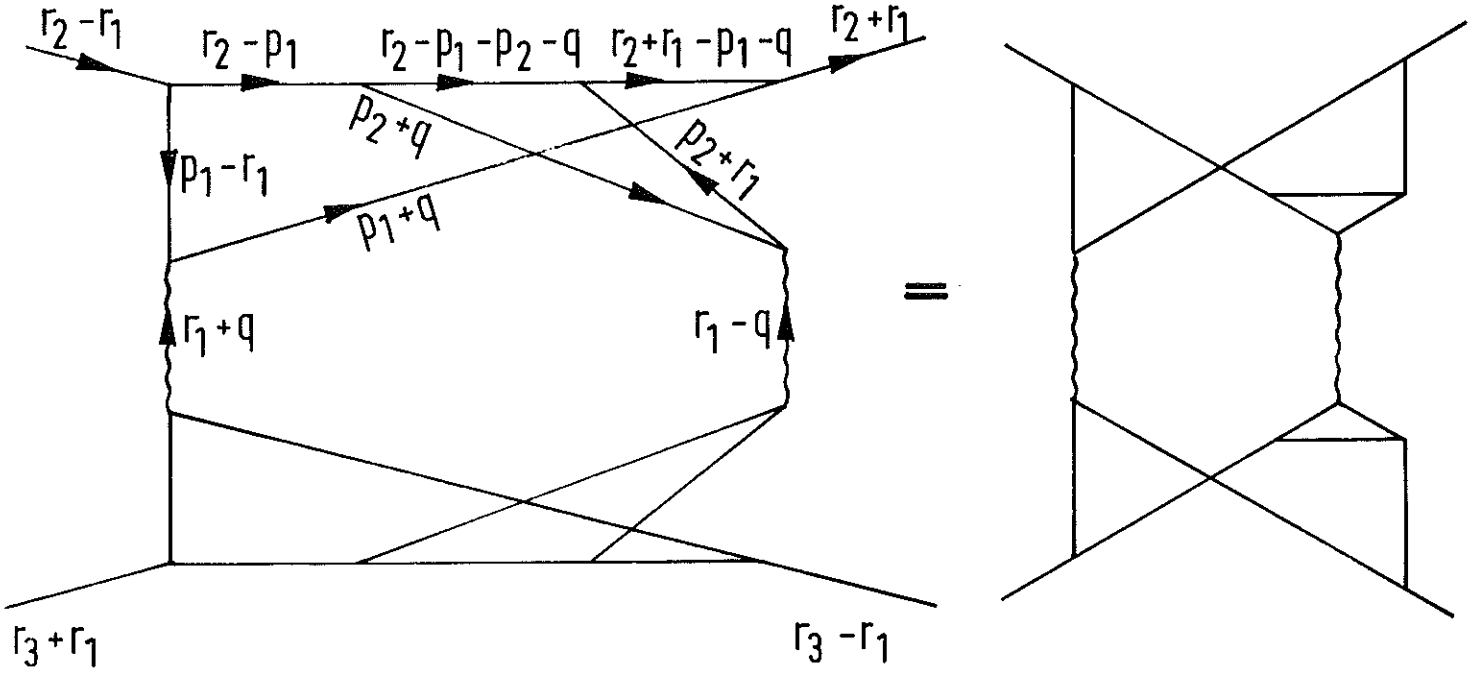
$r_2 - r_1$
$r_2 - p_1$
$r_2 - p_1 - p_2 - q$
$r_2 + r_1 - p_1 - q$
$r_2 + r_1$
$p_2 + q$
$p_2 + r_1$
$p_1 - r_1$
$p_1 + q$
$r_1 + q$
$r_1 - q$
=
$r_3 + r_1$
$r_3 - r_1$

Fig. 2a

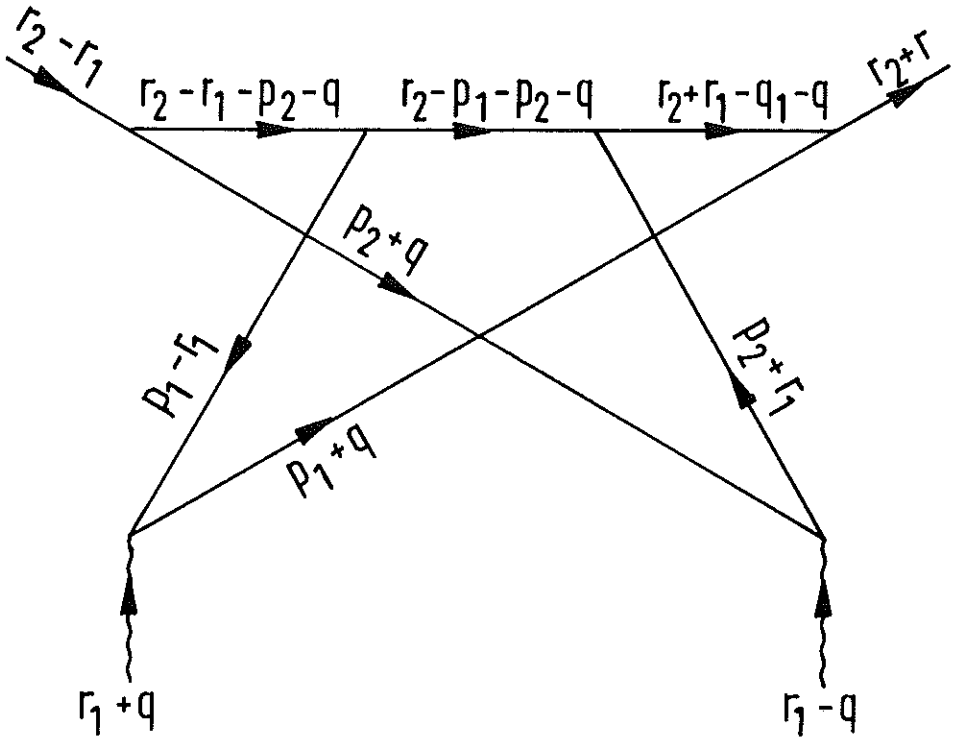

Fig. 2b

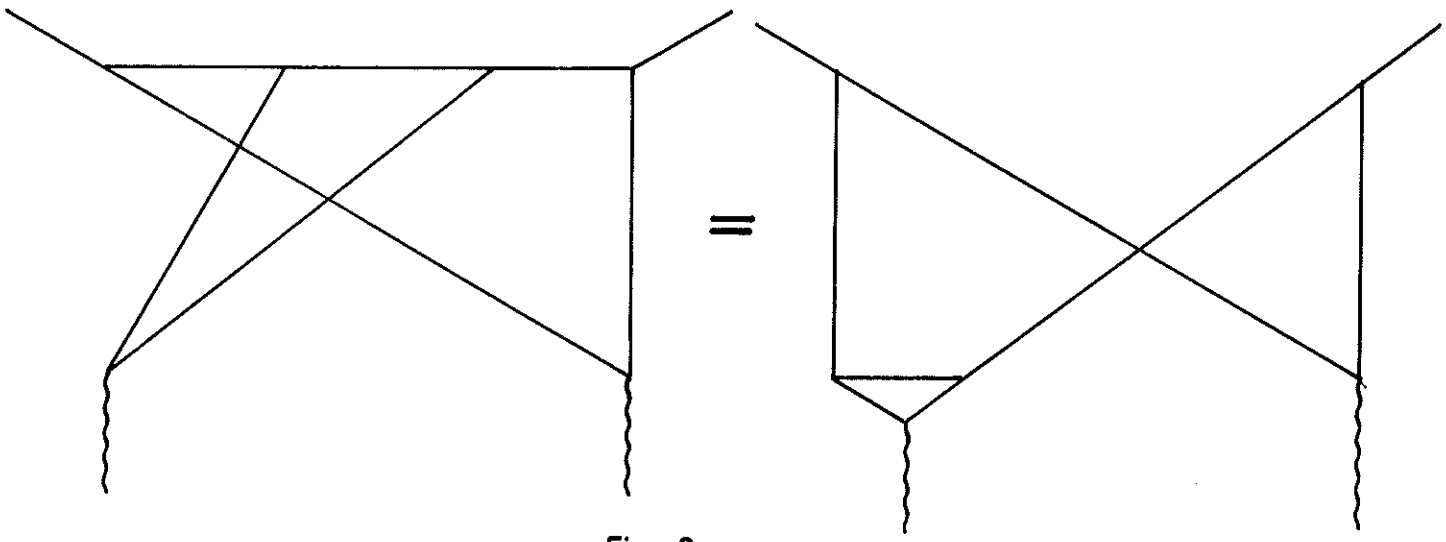

Fig. 2c

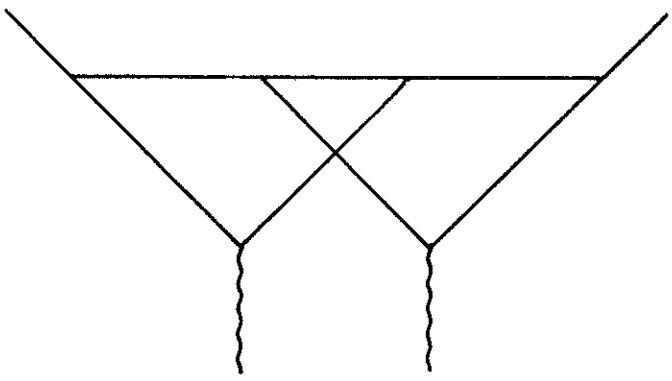

Fig. 2d

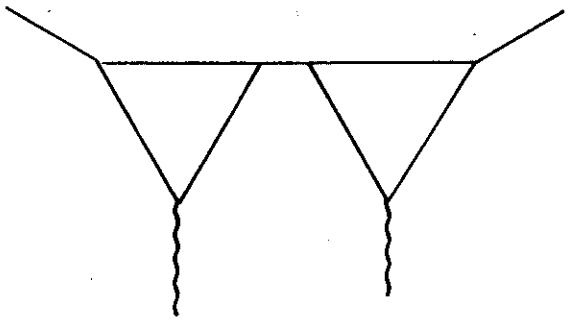

Fig.3

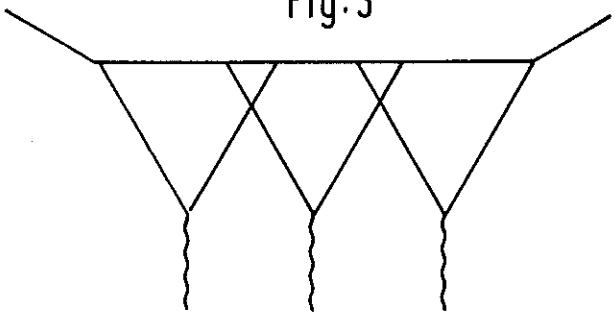

Fig.4

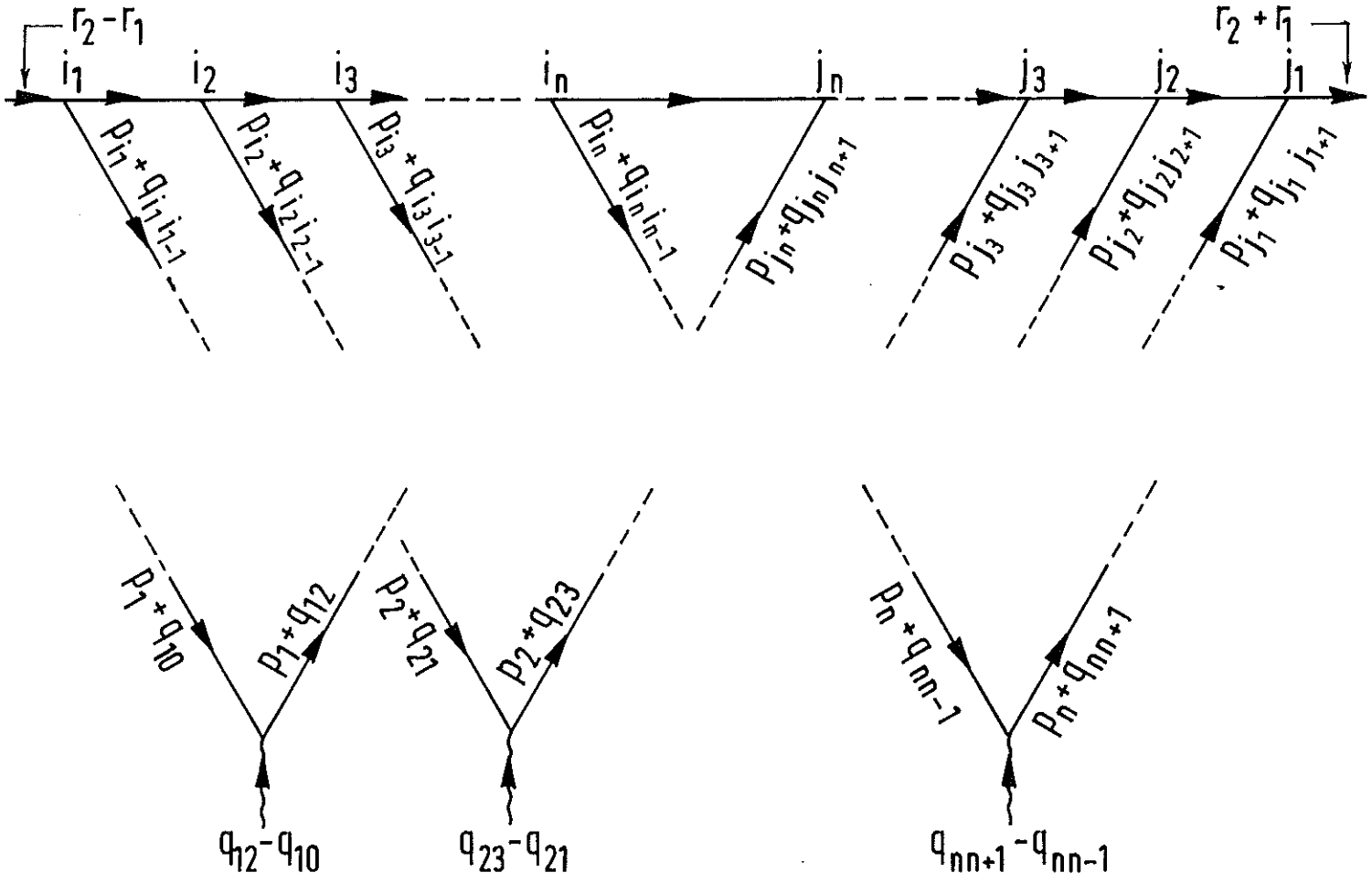

$(q_{ij} = q_{ji}\ ,\ -q_{10} = q_{nn+1} = r_1)$

Fig.5

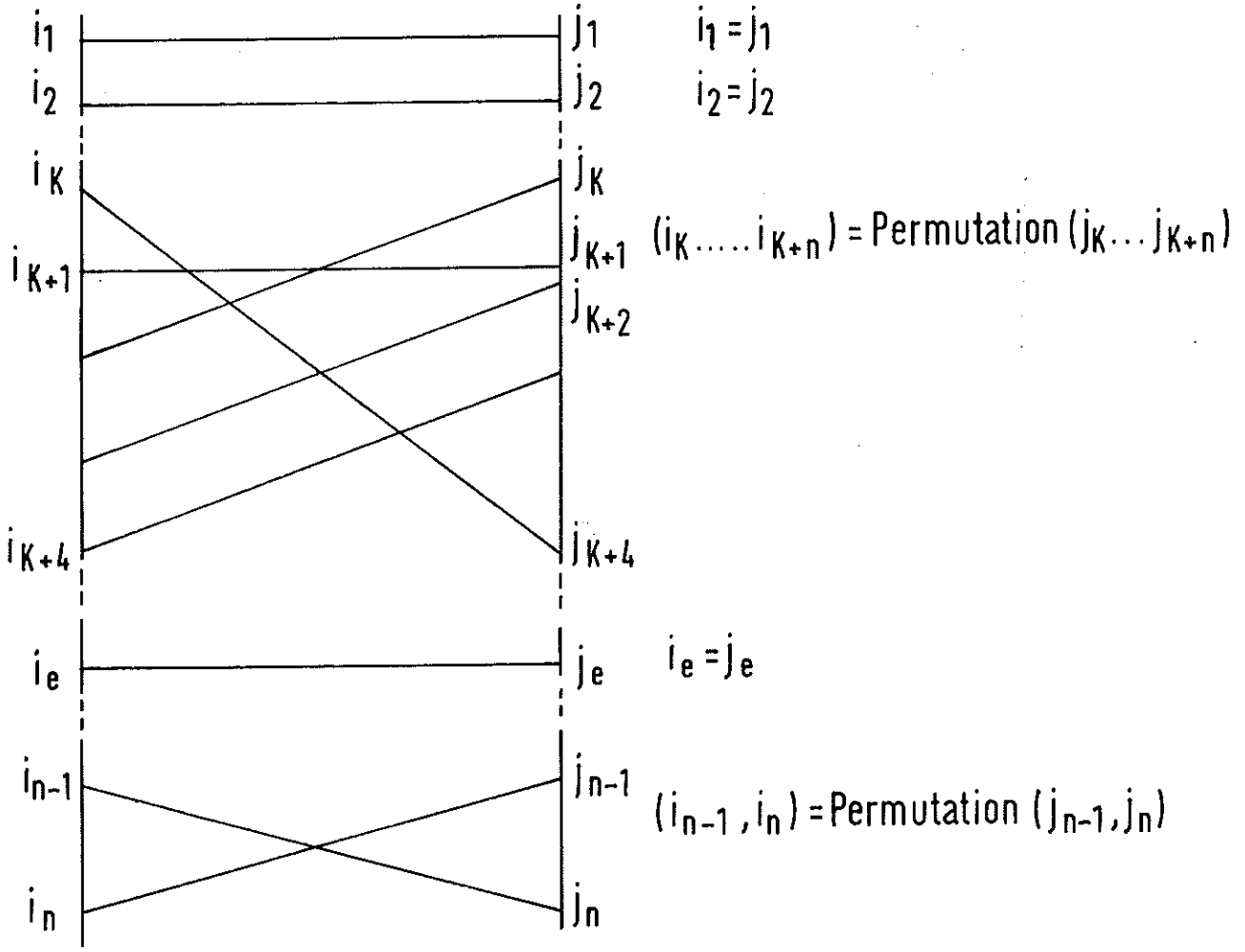
i_1
j_1
$i_1 = j_1$
i_2
j_2
$i_2 = j_2$
i_K
j_K
j_{K+1}
$(i_K \ldots . i_{K+n}) = \text{Permutation}\ (j_K \ldots j_{K+n})$
i_{K+1}
j_{K+2}
i_{K+4}
j_{K+4}
i_e
j_e
$i_e = j_e$
i_{n-1}
j_{n-1}
$(i_{n-1}, i_n) = \text{Permutation}\ (j_{n-1}, j_n)$
i_n
j_n

Fig.6

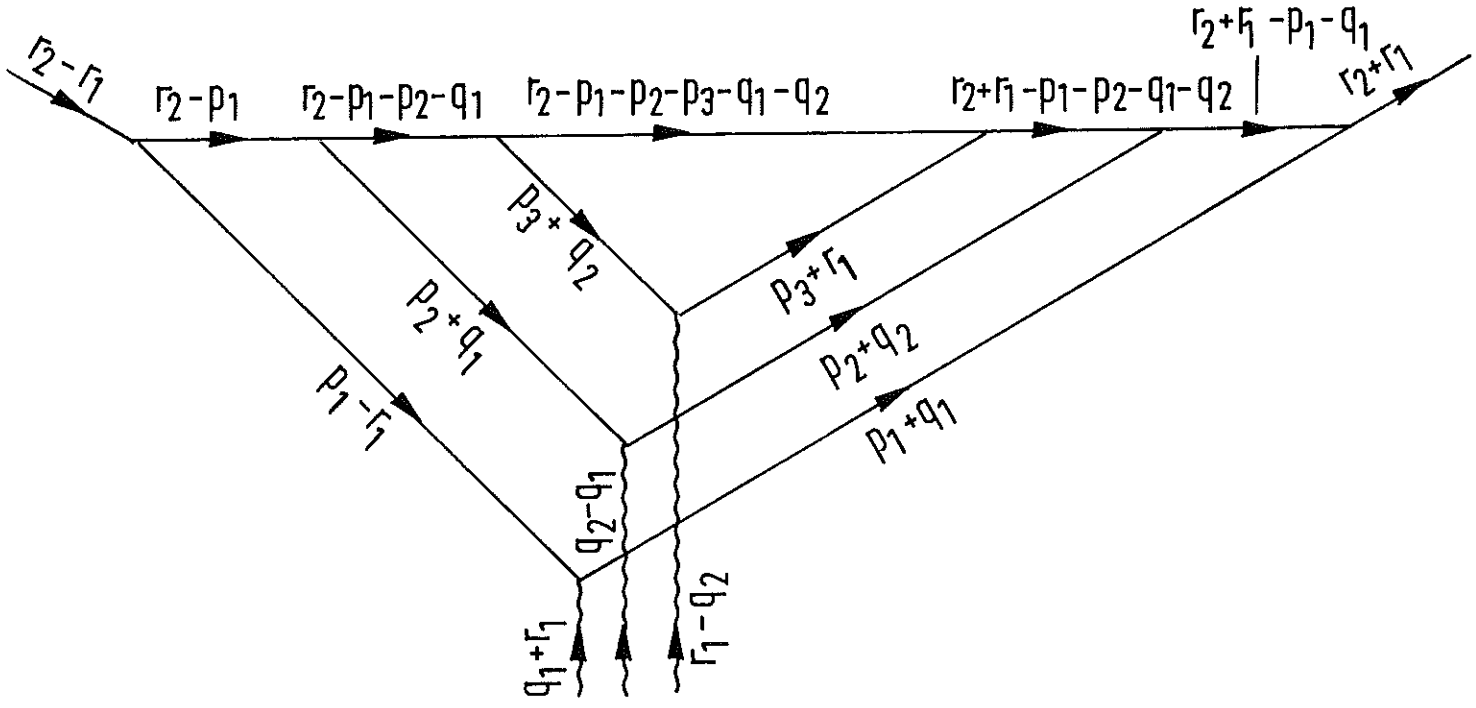
$r_2 - r_1$
$r_2 - p_1$
$r_2 - p_1 - p_2 - q_1$
$r_2 - p_1 - p_2 - p_3 - q_1 - q_2$
$r_2 + r_1 - p_1 - p_2 - q_1 - q_2$
$r_2 + r_1 - p_1 - q_1$
$r_2 + r_1$
$p_3 + q_2$
$p_2 + q_1$
$p_1 - r_1$
$p_3 + r_1$
$p_2 + q_2$
$p_1 + q_1$
$q_2 - q_1$
$q_1 + r_1$
$r_1 - q_2$

Fig. 7

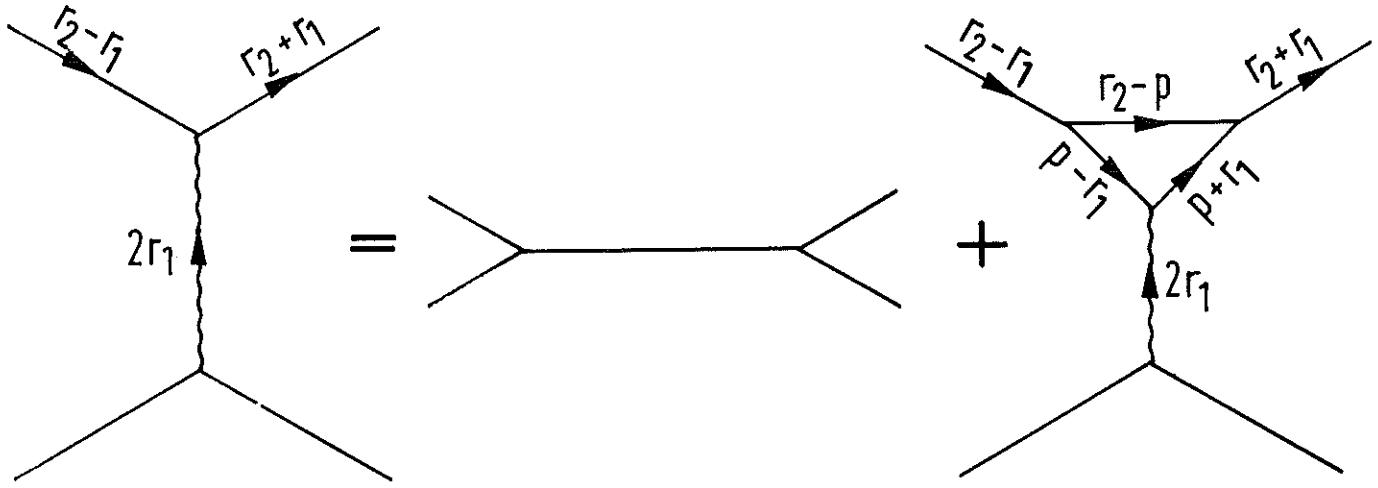

Fig.8